Preparation of Elastomeric Nanocomposites Using Nanocellulose and Recycled Alum Sludge for Flexible Dielectric Materials

Dongyang Sun[1], Bernard L.H. Saw[2], Amaka J. Onyianta[3], Bowen Wang[4], Callum Wilson[1], Dominic O'Rourke[1], Chan H. See[1], Carmen-Mihaela Popescu[5], Mark Dorris[1], Islam Shyha[1], Zhilun Lu[1*]

[1]School of Engineering and Built Environment, Edinburgh Napier University, Edinburgh, UK

[2]Lee Kong Chian Faculty of Eng. and Sci., Universiti Tunku Abdul Rahman, Kajang, Malaysia

[3]Bristol Composites Institute, School of Civil, Aerospace and Mechanical Engineering, University of Bristol, University Walk, Bristol, BS8 1TR, UK

[4]School of Engineering and Materials Science, Queen Mary University of London, London, UK

[5]Petru Poni Institute of Macromolecular Chemistry of the Romanian Academy, Iasi, Romania

[*]Correspondent author

Abstract

Flexible dielectric materials with environmental-friendly, low-cost and high-energy density characteristics are in increasing demand as the world steps into the new industrial 4.0 era. In this work, an elastomeric nanocomposite was developed by incorporating two components: cellulose nanofibrils (CNF) and recycled alum sludge, as the reinforcement phase and to improve the dielectric properties, in a bio-elastomer matrix. CNF and alum sludge were produced by processing waste materials that would otherwise be disposed to landfills. A biodegradable elastomer polydimethylsiloxane was used as the matrix and the nanocomposites were processed by casting the materials in petri dishes. Nanocellulose extraction and heat treatment of alum sludge were conducted and characterised using various techniques including scanning electron microscopy (SEM), thermogravimetric (TGA/DTG) and X-ray diffraction (XRD) analysis. When preparing the nanocomposite samples, various amount of alum sludge was added to examine their impact on the mechanical, thermal and electrical properties. Results have shown that it could be a sustainable practice of reusing such wastes in preparing flexible, lightweight and miniature dielectric materials that can be used for energy storage applications.

Keywords: Nanocellulose, Biodegradable, Sustainable, Alum sludge, Nanocomposite, Flexible, Dielectric.

1. Introduction

Elastomers are an important classes of polymeric materials in which the molecules are lightly cross-linked to form an amorphous structure. They typically undergo large elastic deformation under a small force and therefore have a low Young's modulus and very high elongation at break when compared with other polymers [1]. Some recent research has been reported on the generation of elastomeric

nanocomposites with the incorporation of nano-fillers which has led to the enhancement of their properties significantly. These include the change of optical properties and colour; the improvement of structural stability and surface characteristics; modification of thermal, magnetic, and electrical properties and the improvement of mechanical properties [2]. Various nanosized fillers in the form of fibre, whisker and particle have been investigated, for example carbon fibre [3], chitin whisker [4] and layered clay [5]. Over the past few decades, with increasing focus on environmental issues such as climate change, severe environmental pollution and the depletion of fossil fuels and other resources, the use of wood based cellulosic materials as fillers or reinforcements to replace the conventional fillers in elastomeric composites has attracted great attention [6].

Cellulose, a naturally occurring polymer, is a polysaccharide consisting of linear chains of D-glucose units [7]. It is a key structural component in many higher plants, for example tree, hemp, wheat straw and bamboo. In cellulose structure, elementary units align to form larger bundles of microfibrils and ultimately a cellulosic fibre matrix, complexed with further polymers hemicellulose and lignin bound to the cellulose surface and entrapped within the microfibrils [8]. As nanoscience and nanotechnology develop, the extraction of cellulose nanomaterials using various methods has been widely reported [9, 10]. Nanocellulose is used as a key component for preparing nanocomposites because of its high modulus, strength and lightweight properties, as well as its inherent biodegradable and biocompatible characteristics [11]. Therefore, the addition of such a nanosized reinforcement to elastomers would achieve a more sustainable elastomeric nanocomposite with tailored properties of high specific modulus and specific strength yet flexibility and processibility for various applications.

The work presented in this paper uses a common floating plant, water hyacinth (Eichhornia crassipes) as the feedstock from which to derive cellulose nanofibrils (CNF) as the key reinforcement for the nanocomposites. Water hyacinth is considered an invasive species: it colonises water bodies at a rapid pace, blocking sunlight and reducing oxygen levels in the local ecosystem [12]. Huge sums of money are being spent worldwide to selectively remove the weeds by manual harvesting and use them as animal feed or for energy production by direct combustion [13]. However, it is worth investigating the feasibility of using water hyacinth as feedstock for nanocellulose processing due to their high cellulose content.

The matrix used to form the elastomeric nanocomposite is a biodegradable elastomer, acetoxy-polydimethylsiloxane (PDMS). PDMS are used in wide applications including biomedical engineering [14], energy harvesting [15] and micro-manufacturing [16], exploiting its distinctive characteristics of flexibility, biocompatibility, optical transparency, chemical and thermal stability and ease of manufacturing [17]. A fixed weight ratio of PDMS and CNF was used to prepare the composite.

The key application targeted for the above nanocomposites is to be as flexible dielectric materials for energy storage. Dielectric materials have characteristics of high energy storage density, low loss and

good cycle stability, which are greatly desired in energy storage applications such as electric vehicles, portable electronic devices, and renewable energy systems. As automation and data exchange help define manufacturing in the new Industry 4.0 era [18], portable electronic technology and wearable technology are all in a rapid expansion stage, sharing common features of flexibility, integration, miniaturisation and intellectualisation [19]. Wearable technology incorporates lightweight, smart electronic devices that are worn close to and/or on the surface of the skin, where they detect, analyse and transmit information from the user to the external device [20]. This can facilitate applications including health monitoring [21] and human-machine interaction [22]. Traditional ceramic dielectric materials for energy storage are unable to meet the requirements of lightweight, flexibility and miniaturization in the above applications. As a result, research has focused on processing novel dielectric materials that combine good dielectric properties with lightweight, flexible, low-cost, multifunctional properties, good mechanical performance and high-energy-efficiency characteristics [23, 24]. PDMS has been used with nanoparticle reinforcements such as polymer nanowire [25] and $SrTiO_3$ nanoparticles [26] to form flexible dielectrics. However, using sustainable materials like CNF in PDMS for the same application is less well studied and so forms the basis for this work.

The addition of another component, alum sludge, was also investigated for its impact on the thermal, mechanical and electrical properties of the PDMS/CNF composite. The use of alum sludge in this work follows similar waste management principles as for the water hyacinth material. Alum sludge is a by-product of a water treatment process in which aluminium sulphate is prevalently used as the primary coagulant [27]. According to the data from a project partner-Scottish Water, there are approximately 10,000 tonnes of alum sludge generated from water treatment work landfilled every year in Scotland. The industry has been facing escalating financial and environmental pressure to develop more sustainable strategies to deal with alum sludge wastes. In the available literature, some work of utilising alum sludge has been reported e.g. aluminium recovery or agriculture and land reclamation [28]. However, little work can be found of applying it in processing energy materials for enhanced energy density and efficiency. Therefore, the work has focused on the pre-treatment of the alum sludge and its addition to the PDMS/CNF composites at various loading. The impact on the thermal, mechanical and electrical properties of the composites will also be investigated to see if a more sustainable solution for processing flexible dielectric materials of high performance can be achieved.

2. Materials and Methods

2.1. Materials

Water hyacinth (WH) stems were harvested from a lake in Taman Tasik Seri Aman, Puchong, Malaysia. The WH stems were carefully separated from the roots and leaves, washed and air dried for 3 days before being ground into smaller size as raw materials for preparing the CNF (**Figure 1a**). Dewatered alum sludge was obtained directly from a local water treatment plant of Scottish Water (the Scottish

Water Rosebery Water Treatment Works, Midlothian, Scotland). The average water content of the dewatered sludge was found to be approximately 76% (**Figure 1b**).

Sodium hypochlorite solution (NaClO, 6-14% active chlorine), heptane ($CH_3(CH_2)_5CH_3$, 99%) and sodium hydroxide (NaOH) were received from Sigma-Aldrich, UK. Glacial acetic acid (CH_3COOH) was received from Fisher Scientific, UK. The biodegradable elastomer of acetoxy-polydimethylsiloxane (PDMS, Eastosil E43) was received from Wacker Chemicals Ltd., UK. All chemicals were used without further purification.

2.2. Processing Methods

The major experimental procedures involved in this work can be categorised into three parts: heat treatment and refinement of alum sludge, the processing of CNF, and the forming of cellulose/alum sludge composites in PDMS matrix.

2.2.1. Heat treatment of alum sludge

The dewatered sludge was firstly dried in an oven over a period of 24 hours at 105°C before being further processed. Once dried, the resulting crumb particle size was reduced using a planetary ball mill. Sieve separation was used and particles smaller than 250µm were retained. Particles larger than this were returned to the ball mill for further processing until all material passed through a 250µm mesh. The sieved material was then heat treated in a box furnace for 7 hours at 300°C, 800°C, 1300°C and 1500°C using a heating rate of 50°C/min and left to cool overnight to degrade thermally unstable materials. This experiment was to determine a suitable heat treatment temperature for the sludge powder to be prepared and used in the subsequent composite forming work.

2.2.2 Cellulose nanofibril processing

A simple and less energy intensive method was used to process CNF as adapted from the previous work [29]: dried water hyacinth was soaked in water to form slurry before being subjected to a delignification process using NaClO solution. Additionally, the material was processed in 1% NaOH solution to continue the extraction process. Both reactions were completed at room temperature and the material was washed using ultrapure water after each chemical reaction. Upon the completion of the above, a 0.5% cellulose slurry was prepared. To obtain nanofibrils, the cellulose slurry was further treated in a high shear homogeniser (PSI-20, Adaptive Instruments, UK) by passing it through a 200µm Z-shape interaction chamber for 1 pass, at 700bar. The produced nanocellulose was eventually solvent exchanged from water into heptane to aid the composite forming process. The solid content of the final slurry is approximately 3.5%.

2.2.3 Composite forming

The composites were prepared by first mixing the CNF slurry with the PDMS using 70:30 weight ratio. This value was determined by trials of other ratios (e.g. 80:20 and 60:40 weight ratio), in which they can either be of insufficient PDMS as the matrix or excessive PDMS to obstruct the flowability of the mixture. The mixing was completed in heptane solvent in order to achieve a free flow condition of the mixture. Subsequently, the alum sludge powder that was heat treated at 800°C was added to the mixture. The weight % of the alum sludge powder with respect to the mixture was 10%, 15% and 20%, respectively. The mixture of approximately 40g in weight was vigorously mixed using an acoustic mixer (LabRAM, Resodyn, USA) and a rotor stator mixer (T 25 digital ULTRA-TURRAX, IKA, UK), in order to achieve a good dispersion. The mixture was cast in a petri dish and left to cure at ambient condition. Finally the dried film was removed from the mould and denoted as PDMSCNF, PDMSCNF10AS, PDMSCNF15AS and PDMSCNF20AS, for the composite samples with 0%, 10%, 15% and 20% alum sludge, respectively.

2.3 Characterisation

2.3.1 Characterisation of CNF and alum sludge

The morphological features of the CNF and alum sludge samples were examined using scanning electron microscopy (FESEM, Hitachi, UK). Thermogravimetric analysis and its derivative (TGA/DTG), was conducted on the raw alum sludge crumb (before being heat treated) using Netzsch simultaneous thermal analyser, STA 449 (Netzsch, Germany). 20-25 mg of each sample was heated in an aluminium oxide pan from 30 to 900 °C at a heating rate of 10 °C min^{-1} under a constant nitrogen of 50 mL min^{-1}. DTG curves were obtained by performing a first derivative on the % weight loss data from TGA using Origin 2020b version.

The X-ray diffraction patterns were recorded with a Bruker D8 Advance X-ray diffractometer (Germany) by using Cu-K radiation (λ = 0.1542 nm), a parallel beam with Gobel mirror and a Dynamic Scintillation detector. The accelerating voltage was of 40 kV, the current of 30 mA and scanning range between 5° and 40° (2theta).

2.3.2 Characterisation of composite films

The morphology of the composite films was examined using the SEM. Mechanical testing was completed to investigate the strength and ductility properties of the composite. A universal testing machine was used for this test in which the material was pulled to break at a rate of 50mm/min. 12 specimens were prepared for each sample, using which the mean values and standard deviation of tensile strength and % elongation at break were calculated, respectively.

The thermal properties of the four composite films were examined using the above TGA/DTG instrument and the same test conditions. For dielectric and energy storage properties, the samples were coated with silver paste (Johnson Matthey, No. E110) on both sides of the film. Frequency-dependent

permittivity and dielectric loss in the frequency range of 30 Hz to 1 MHz were measured using a precision LCR metre model, Agilent 4184A. The polarization-electric field (P-E), and current-electric field (I-E) loops of coated samples were measure by the ferroelectric hysteresis measurement tester (NPL, UK) at 10 Hz.

3. Results and Discussion

CNF were successfully obtained using both chemical and mechanical steps. In the first step, lignin was removed in the acidified NaClO solution, followed by the removal of hemicellulose in the NaOH solution. This can be observed by colour change in the material (from dark brown to white) in the process. The resultant material was then subjected to high shear processing to fibrillate the material into nanofibrils. **Figure 2** shows the microstructure of high aspect ratio CNF obtained from the above process. The long nature of the fibrils results in formation of a web-like network structure, similar to that observed in other published works [30]. The enlarged image in **Figure 2 b)** clearly shows the morphology of individual fibrils, which can be estimated as approximately 20nm in diameter. Due to the entangled nature of the fibrils, it is not possible to measure their length accurately; however, it can be estimated from **Figure 2 a)** that they can be in the order of several micrometres long.

It is also evident from the circularly highlighted area in **Figure 2 a)** that a small proportion of larger unfibrillated fibre bundles were present, having a diameter of approximately several hundred nanometres. This could be the result of the incomplete fibrillation of material during the homogenisation step. Previous work has shown that the degree of fibrillation is determined by various aspects, including the nature of the feedstock, processing time and the amount of shear force applied on the materials; the latter two aspects are directly correlated to the amount of energy consumed in the process. In this work, the material was processed using a 200 µm interaction chamber for 1 pass (1 cycle), which shows a significant improvement in energy consumption efficiency than in previous work where the material is passed through a 100µm chamber for up to 5 cycles. Subsequent experiments in this work have identified that the processed material is suitable for the composite forming process.

The TGA/DTG thermogram elucidating the thermal stability of the raw alum sludge crumb is shown in **Figure 3 a)**. A noticeable amount of weight (approximately 46%) has been lost when the sample was heated up to 900°C. Three steps can be seen in the weight loss profile: i) up to 100°C, approximately 4% of weight is lost, which could mainly be associated to the physically absorbed moisture (remaining free/unbound water in the porous structure of unheated sludge sample that can be seen in **Figure 3 b**). ii) There is a major weight loss between 105°C and 500°C. This loss could possibly be because of the removal of the remaining bonded water and the decomposition of some organic compounds (e.g. polyaluminium chloride hydroxide sulphate, one of the key components in the sludge, usually decomposes at about 200°C [31]). It is reported that the decomposition of polyacrylamide, an anionic organic polymer (e.g. Magnafloc®) that is commonly used to improve the dewatering of alum sludge

in the water treatment process, can occur in between 350°C and 550°C [32]; this could be another aspect for the above weight loss in our work. iii) Above 500°C, the curve started plateauing, showing insignificant weight loss in this range. All these observations are correlated with the thermal event shown in the DTG curve in the same temperature range. In summary, the alum sludge used in this work contains various compounds that are thermally unstable; thus, it is necessary for them to undergo some heat treatment to remove the volatile substances before being used in forming the composites.

The XRD patterns of untreated alum sludge and samples with various heat treatments are shown in **Figure 4**. Due to the large background signal, the crystallinity of the raw alum sludge is quite poor, and it is difficult to identify a distinct peak. The spectrum for the 300°C shows a peak for hexagonal quartz SiO_2. When the sample was heat treated at 800°C, more peaks can be seen which could be associated to cubic γ-Al_2O_3. Similar results have been reported elsewhere [33, 34] and these structures could possibly be formed in the oxidation process at the elevated temperatures. A broader peak in the spectrum at 800°C indicates that the sample is of low crystallinity at this stage in comparison with heat treatment at 1300°C and 1500°C, at which the peaks became sharper and more numerous. These peaks may be associated with orthorhombic corundum Al_2O_3 and mullite Al_6SiO_{13}. Since no significant difference can be seen between the two spectra of 1300° and 1500°, it is believed that from 1300°C, the compound has achieved its crystalline phase. Based on the results in **Figure 3** and **Figure 4**, it is reasoned that alum sludge heat treated at 800°C developed an oxide structure with reasonable thermal stability and is thus suitable for use in the formation of composites. Although the heat treatment at 1300° and 1500° would result in a material of higher crystallinity, particle coalescence would make the sample nonhomogeneous and difficult to disperse in the matrix when preparing the composites.

A representative SEM micrograph showing the morphology of the PDMSCNF10AS film can be seen in **Figure 5 a)**. Alum sludge particles appear embedded in the matrix with a broadly even distribution, although clusters of smaller particles are evident, shown in more morphological detail in the enlarged image in **Figure 5 b)**. An image with greater magnification (**Figure 5 c)** shows the CNF is also embedded in the PDMS matrix homogeneously with random orientations. The CNF structure can be recognised as identical when compared with the one shown in **Figure 2**. The microstructure of other film samples was similar to PDMSCNF10AS (except of the different content of alum sludge particles) and these are not shown.

The strength and % elongation at break obtained from the mechanical tests on composite samples are summarised in **Figure 6**. It can be seen that the addition of alum sludge has adversely affected the tensile strength of the composites: the PDMSCNF composite with no alum sludge has a tensile strength of approximately 0.65MPa, but this reduces to roughly 1/3 with 20% alum sludge. This may be attributed to particle heterogeneity and poor interfacial bonding between the particles; the PDMS matrix thus providing a weak point of the material when under external stress. During the preparation of the

composite mixture, the compound was always of high viscosity, especially when the alum sludge content was increased. This made it difficult to homogenise the components and may have resulted in uneven local dispersion in the composite film: a possible contributory factor in lowered tensile strength and greater standard deviation in sample sets. An increase in volume fraction of particles to enhance stiffness in a polymer matrix composite may be expected to decrease toughness/flexibility and this is confirmed by elongation at break data, shown in **Figure 6 c).** The PDMSCNF composite under stretch shows the flexibility of the polymer matrix with cellulose fibre reinforcement. The reduction of % elongation at break broadly correlates with volume fraction of the alum sludge in the composite, a trend apparently bucked by the data for PDMSCNF10AS which shows higher elongation at break than the PDMSCNF sample without alum sludge. Standard deviation is however comparatively high in these two sample sets and the data may be significantly improved by increasing the sample size and optimising experimental conditions for improved particle homogeneity, dispersion and interfacial interactions with the matrix.

Thermal stability studies were carried out and the results overlayed in the thermogravimetric analysis (TGA, **Figure 7a**) and derivative thermogravimetric (DTG, **Figure 7b**) curves for the four PDMSCNF composites with various alum sludge content. The TGA graph shows a relatively flat line below 300°C, indicating minimum weight loss due to solvent evaporation. Two degradation troughs can be observed at around 300°C and 550°C in the associated TGA and DTG curves. These are assigned to the degradation of CNF and PDMS, respectively. As the content of alum sludge increases, the degradation temperatures for CNF and PDMS are affected differently (**Figure 7b**): the peak degradation temperatures of CNF were shifted to higher temperatures, while the peak degradation temperatures of PDMS shifted to slightly lower values. This is more pronounced in the PDMSCNF15AS and PDMSCNF20AS samples, indicting that greater amount of alum sludge affected the degradation temperatures more significantly.

It is worth noting that the addition of alum sludge at different weight loadings to the composites increased the amount of char remaining at 600-900°C. Char formation is a desired property required for fire-retardant composite materials. The high residual char of these composites make them desirable in electrical devices which are prone to short-circuiting [35]. The increased amount of alum sludge in the composite could improve the fire-retardant property of the composite when they are used in energy storage applications.

Figure 8 shows the frequency dependence of the dielectric constant and dielectric loss for the PDMSCNF composite films with various alum sludge content. In the frequency range of 30 Hz to 1 MHz, the dielectric constant drops gradually as frequency increases. This drop is due to the diminishing influence of dipolar polarization. As the alum sludge content increases, the dielectric constant of the

PDMSCNF composite films rises, which is because of the greater dielectric constant of Al_2O_3 and mullite-based sludge (6.7-10) compared to pure cellulose (2-4) at this frequency range [36-38].

Figure 9 displays the P-E and I-E loops of the composite samples to explore the energy storage properties. In the same electric field, as the amount of the alum sludge increases, polarizability increases and electrical resistivity decreases. The rise in polarizability is consistent with the measured dielectric constant as shown in **Figure 8 a)**. This is owing to the presence of comparatively high dielectric constant of the alum sludge. Moreover, the reduction in electrical resistivity may not be due to intrinsic factors, but rather to poor adhesion between the electrode and the composite films with the alum sludge in the high electric fields. This coincides with the observation in **Figure 8 b)** that the dielectric loss of PDMSCNF at low frequencies is higher than the PDMSCNFAS films. These film samples will need enhanced silver paste electrodes in the future, which will result in a larger applied electric field and thus a greater energy storage property.

4. Conclusions

This work has demonstrated the use of waste materials to reinforce nanocomposites for flexible dielectric materials. Two waste material sources were used; dried water hyacinth and alum sludge and these were mixed with a biodegradable elastomer PDMS matrix. A simple and less-energy intensive method was used to extract CNF from dried water hyacinth and the as received alum sludge was heat treated and refined to be suitable for the composite forming process. The results showed that incorporating these reinforcements into a polymer matrix to produce a functional composite is possible and that the addition of alum sludge particles in the PDMS/CNF composite has significant effects on the material properties of the composite. Mechanical, thermal and electrical properties are differentially affected by alum particle reinforcement, allowing a tailored approach to maximise desirable features while compromising less desirable ones for any specific application. This work has provided a strong basis for showing the potential of reusing waste materials in preparing flexible, lightweight and miniature dielectric materials that can be used for sustainable energy storage applications.

Acknowledgments

This project is supported by a Research Environment Links Grant No. MIGHT/CEO/NUOF/1-2022 (2) from the British Council and Malaysia Industry-Government Group for High Technology, as part of the British Council's Going Global Partnerships programme. The programme builds stronger, more inclusive, internationally connected higher education and TVET systems. The authors also would like to thank Ms Lynn Chalmers for her support in the experimental works.

References

1. Gupta, T., U. Kulshrestha, and S. Bandhu Ghosh, *Green elastomeric nanocomposites for high-performance applications.* Materials Today: Proceedings, 2020. **28**: p. 2494-2497.

2. Mittal, V., J.K. Kim, and K. Pal, *Recent advances in elastomeric nanocomposites*. Vol. 9. 2011: Springer.
3. Thomas, A. and J. Whittle, *Tensile rupture of rubber.* Rubber Chemistry and Technology, 1970. **43**(2): p. 222-228.
4. Gopalan Nair, K. and A. Dufresne, *Crab Shell Chitin Whisker Reinforced Natural Rubber Nanocomposites. 2. Mechanical Behavior.* Biomacromolecules, 2003. **4**(3): p. 666-674.
5. LeBaron, P.C. and T.J. Pinnavaia, *Clay Nanolayer Reinforcement of a Silicone Elastomer.* Chemistry of Materials, 2001. **13**(10): p. 3760-3765.
6. Zhou, Y., et al., *Lignocellulosic fibre mediated rubber composites: An overview.* Composites Part B: Engineering, 2015. **76**: p. 180-191.
7. Updegraff, D.M., *Semimicro determination of cellulose inbiological materials.* Analytical Biochemistry, 1969. **32**(3): p. 420-424.
8. ROBERTS, J., *Srivastava, L. M. Plant growth and development. Hormones and the environment.* Annals of Botany, 2003. **92**(6): p. 846-846.
9. Istirokhatun, T., et al., *Cellulose Isolation from Tropical Water Hyacinth for Membrane Preparation.* Procedia environmental sciences, 2015. **23**: p. 274-281.
10. Mahardika, M., et al., *Production of Nanocellulose from Pineapple Leaf Fibers via High-Shear Homogenization and Ultrasonication.* Fibers, 2018. **6**(2): p. 28.
11. Phanthong, P., et al., *Nanocellulose: Extraction and application.* Carbon Resources Conversion, 2018. **1**(1): p. 32-43.
12. Mitan, N.M.M. *Water hyacinth: Potential and Threat*. in *International Conference on Chemical Sciences and Engineering (ICCSE) - Advance and New Materials*. 2018. Melaka, MALAYSIA.
13. Gunnarsson, C.C. and C.M. Petersen, *Water hyacinths as a resource in agriculture and energy production: a literature review.* Waste Manag, 2007. **27**(1): p. 117-29.
14. Ceseracciu, L., et al., *Robust and Biodegradable Elastomers Based on Corn Starch and Polydimethylsiloxane (PDMS).* ACS Applied Materials & Interfaces, 2015. **7**(6): p. 3742-3753.
15. Jang, S. and J.H. Oh, *Rapid Fabrication of Microporous BaTiO3/PDMS Nanocomposites for Triboelectric Nanogenerators through One-step Microwave Irradiation.* Scientific Reports, 2018. **8**(1): p. 14287.
16. Chen, X.L., et al., *The Fabrication and Application of a PDMS Micro Through-Holes Mask in Electrochemical Micromanufacturing.* Advances in Mechanical Engineering, 2014.
17. Pereira Sales, F., et al., *Mechanical Characterization of PDMS with Different Mixing Ratios.* Procedia Structural Integrity, 2022. **37**: p. 383-388.
18. Radanliev, P., et al., *Artificial Intelligence and the Internet of Things in Industry 4.0.* Ccf Transactions on Pervasive Computing and Interaction, 2021. **3**(3): p. 329-338.
19. Xu, C., et al., *Portable and wearable self-powered systems based on emerging energy harvesting technology.* Microsystems & Nanoengineering, 2021. **7**(1): p. 25.
20. Düking, P., et al., *Comparison of Non-Invasive Individual Monitoring of the Training and Health of Athletes with Commercially Available Wearable Technologies.* Frontiers in Physiology, 2016. **7**.
21. Memon, S.F., M. Memon, and S. Bhatti, *Wearable technology for infant health monitoring: a survey.* Iet Circuits Devices & Systems, 2020. **14**(2): p. 115-129.
22. Lin, Z.W., et al., *A Personalized Acoustic Interface for Wearable Human-Machine Interaction.* Advanced Functional Materials, 2022. **32**(9).
23. Xu, W., et al., *A stretchable solid-state zinc ion battery based on a cellulose nanofiber–polyacrylamide hydrogel electrolyte and a Mg0.23V2O5·1.0H2O cathode.* Journal of Materials Chemistry A, 2020. **8**(35): p. 18327-18337.
24. Yin, Y., et al., *Flexible cellulose/alumina (Al2O3) nanocomposite films with enhanced energy density and efficiency for dielectric capacitors.* Cellulose, 2021. **28**(3): p. 1541-1553.

25. Du, P., X. Lin, and X. Zhang. *Dielectric constants of PDMS nanocomposites using conducting polymer nanowires*. in *2011 16th International Solid-State Sensors, Actuators and Microsystems Conference*. 2011.
26. Bertasius, P., et al., *Dielectric properties of polydimethylsiloxane composites filled with SrTiO3 nanoparticles.* Polymer Composites, 2021. **42**(6): p. 2982-2988.
27. Babatunde, A.O. and Y.Q. Zhao, *Constructive Approaches Toward Water Treatment Works Sludge Management: An International Review of Beneficial Reuses.* Critical Reviews in Environmental Science and Technology, 2007. **37**(2): p. 129-164.
28. Dassanayake, K.B., et al., *A review on alum sludge reuse with special reference to agricultural applications and future challenges.* Waste Management, 2015. **38**: p. 321-335.
29. Sun, D., et al., *A process for deriving high quality cellulose nanofibrils from water hyacinth invasive species.* Cellulose, 2020. **27**(7): p. 3727-3740.
30. Chen, W., et al., *Isolation and characterization of cellulose nanofibers from four plant cellulose fibers using a chemical-ultrasonic process.* Cellulose, 2011. **18**(2): p. 433-442.
31. Soleha, M.Y., et al., *Characterization of Raw and Thermally Treated Alum Sludge.* Key Engineering Materials, 2016. **701**: p. 138-142.
32. Bache, D.H. and Y.Q. Zhao, *Optimising polymer use in alum sludge conditioning: an ad hoc test.* Journal of Water Supply: Research and Technology-Aqua, 2001. **50**(1): p. 29-38.
33. Owaid, H., et al., *Physical and Mechanical Properties of High Performance Concrete with Alum Sludge as Partial Cement Replacement.* Jurnal Teknologi, 2013. **65**.
34. Awab, H., T. Paramalinggam, and A.R. Mohd Yusoff, *Characterization of Alum Sludge for Reuse and Disposal.* Malaysian J Fund Appl Sci, 2012. **8**: p. 209-213.
35. Prabhakar, M.N., et al., *Hybrid approach to improve the flame-retardant and thermal properties of sustainable biocomposites used in outdoor engineering applications.* Composites Part A: Applied Science and Manufacturing, 2022. **152**: p. 106674.
36. Zhang, L., S. Olhero, and J.M.F. Ferreira, *Thermo-mechanical and high-temperature dielectric properties of cordierite-mullite-alumina ceramics.* Ceramics International, 2016. **42**(15): p. 16897-16905.
37. Groner, M.D., et al., *Electrical characterization of thin Al2O3 films grown by atomic layer deposition on silicon and various metal substrates.* Thin Solid Films, 2002. **413**(1): p. 186-197.
38. Khouaja, A., A. Koubaa, and H. Ben Daly, *Dielectric properties and thermal stability of cellulose high-density polyethylene bio-based composites.* Industrial Crops and Products, 2021. **171**: p. 113928.

Figures and Figure Captions

(a) **(b)**

Figure 1 (a) dried and ground water hyacinth material; **(b)** dewatered alum sludge sample collected from a treatment plant of Scottish Water.

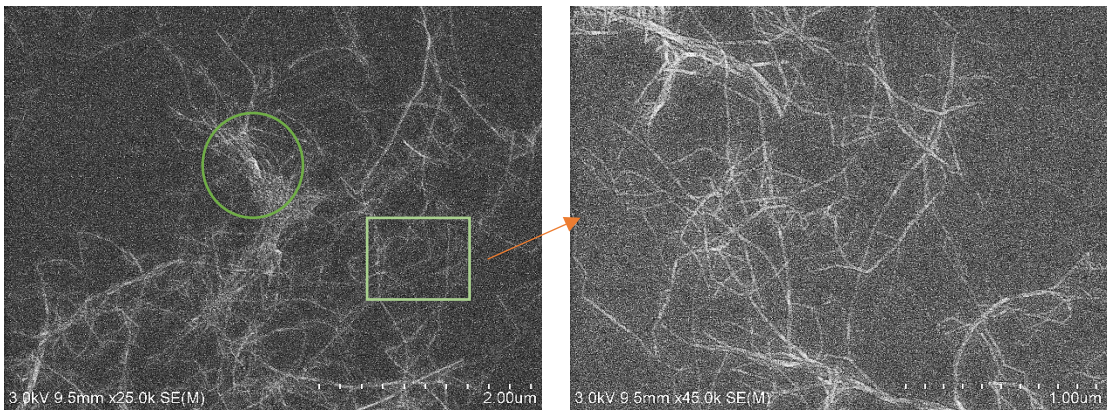

(a) **(b)**

Figure 2 (a) FESEM images of cellulose nanofibrils showing the web-like network structure; the arrow highlights a unfibrillated fibre bundle; and **(b)** the enlarged image of the rectangular area in **(a)**, showing the morphology of individual nanofibrils.

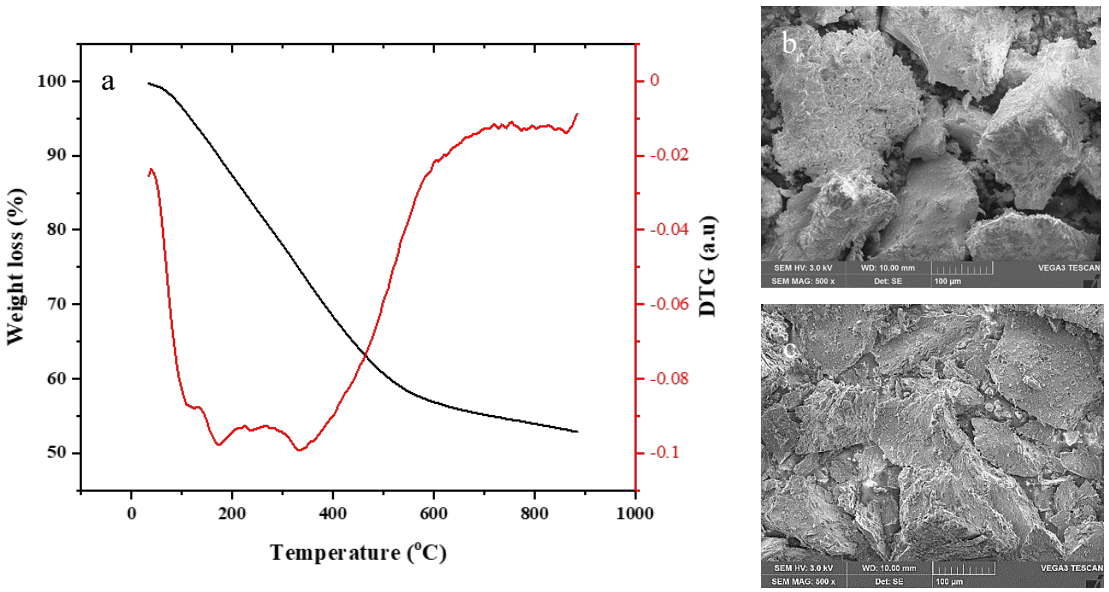

Figure 3 (a) TGA/DTG thermograms of the raw alum sludge; **(b)** the alum sludge without heat treatment and **(c)** the sludge which was heat treated at 800°C.

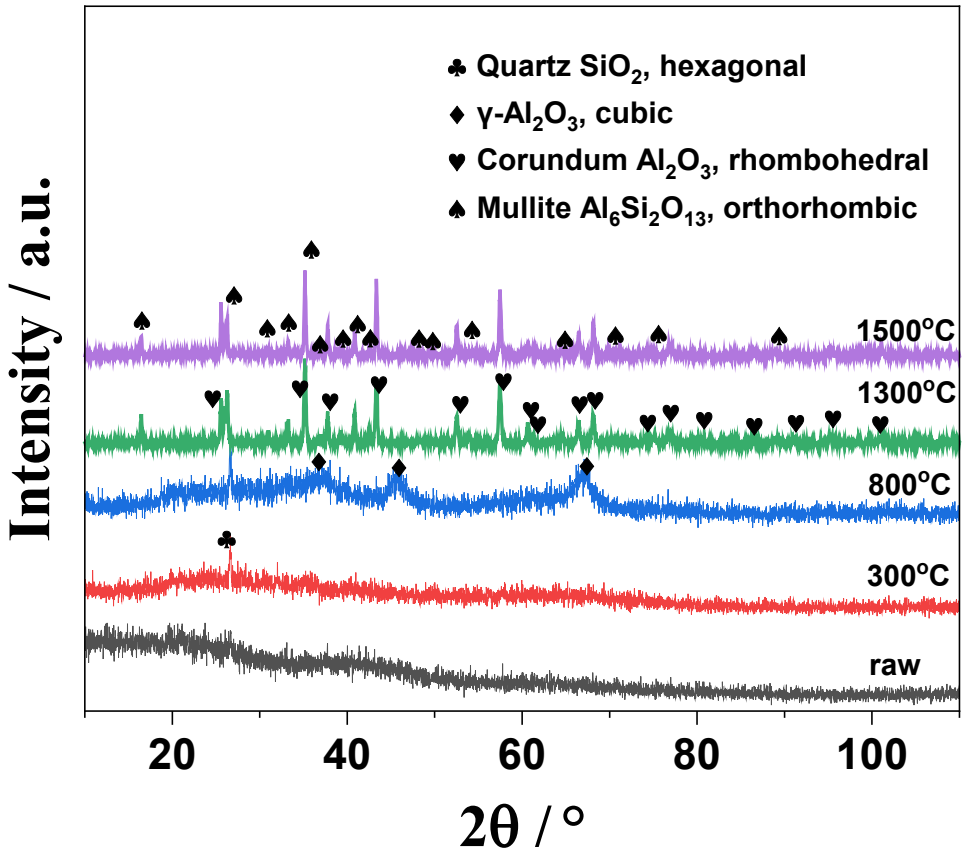

Figure 4 XRD spectra for the raw and heat treated alum sludge samples at 300°C, 800°C, 1300°C and 1500°C, respectively.

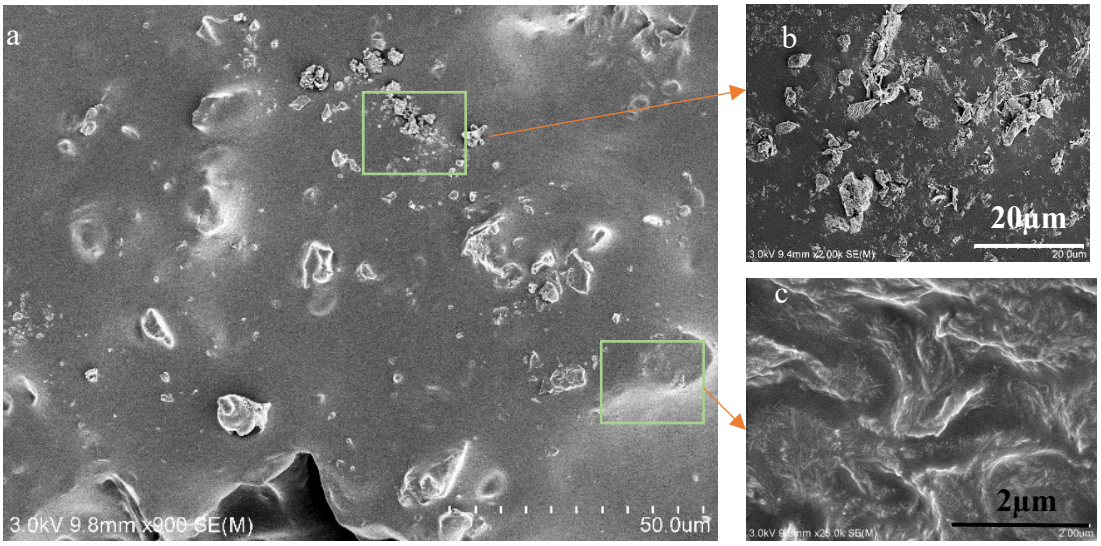

Figure 5 (a) SEM micrograph of cross-sectional structure of the PDMSCNF10AS composite film; **(b)** enlarged image showing the alum sludge particles; **(c)** enlarged image showing the CNF in the matrix.

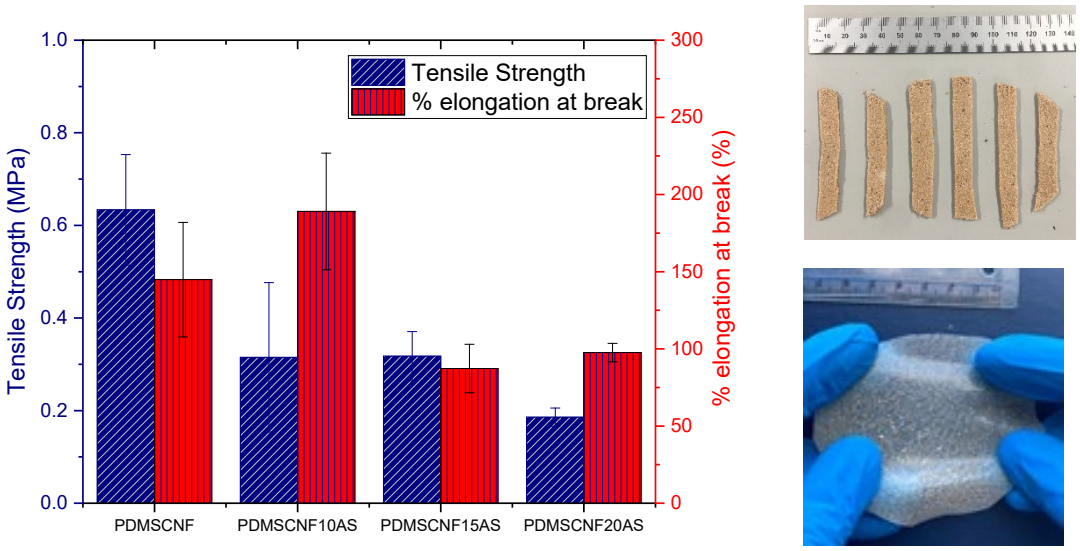

Figure 6 Engineering tensile stress v.s. engineering tensile strain curve for the composite film; the two embedded images show the tensile samples and the composite film before testing.

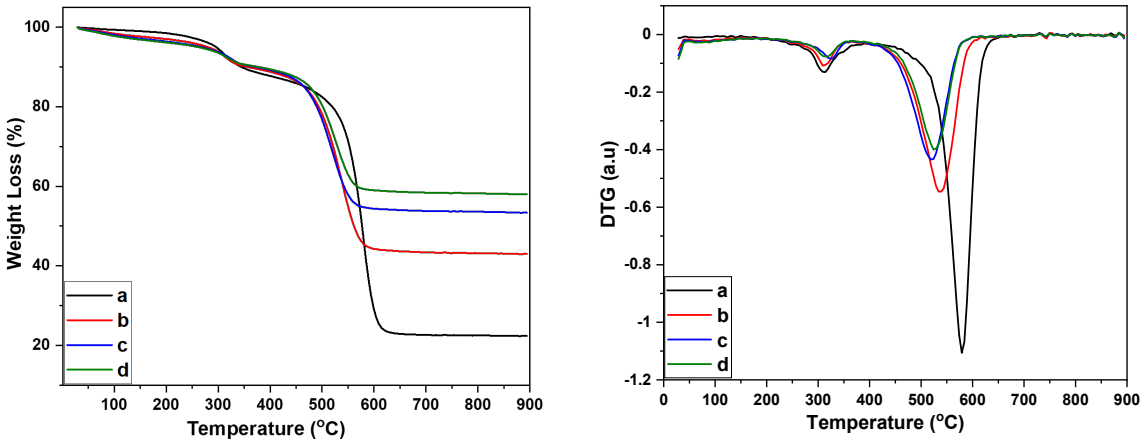

a) **b)**

Figure 7 TGA (a) and DTG (b) thermograms of the PDMSCNF composites with various weight ratio of alum sludge; a-PDMSCNF; b-PDMSCNF10AS; c-PDMSCNF15AS; d-PDMSCNF20AS. The peak degradation temperatures on Figure 7 (b) correspond to the degradation of CNF (~ 300 ºC) and PDMS (~ 550 ºC).

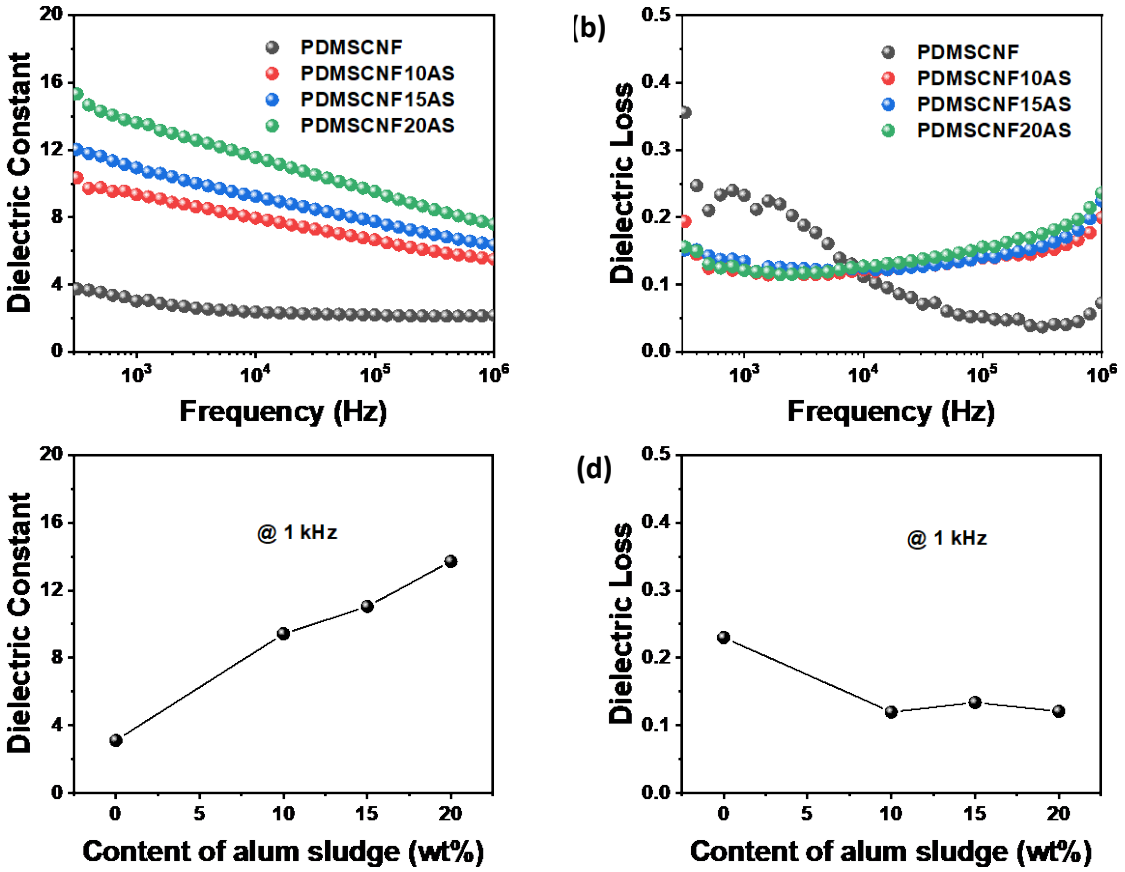

Figure 8 Frequency dependence of the **(a)** dielectric constant and **(b)** dielectric loss for the PDMSCNF composite films with alum sludge; **(c)** dielectric constant and **(d)** dielectric loss measured at 1kHz as a function of the alum sludge content.

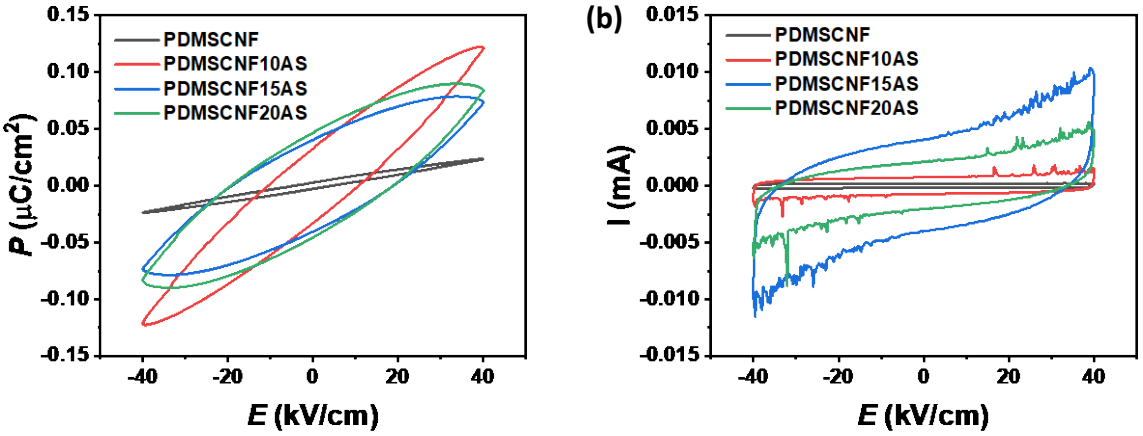

Figure 9 P-E Loop and I-E Loop for the PDMSCNF composites with various content of alum sludge.